Title

Controlling the Oligomerization State of Aβ-Derived Peptides with Light.

Journal

Journal of the American Chemical Society, 140(17)

Authors

Salveson, Patrick
Haerianardakani, Sepehr
Thuy-Boun, Alexander
et al.

Publication Date

2018-05-02

DOI

10.1021/jacs.8b02658

Peer reviewed

HHS Public Access

Author manuscript

J Am Chem Soc. Author manuscript; available in PMC 2019 May 02.

Published in final edited form as:

J Am Chem Soc. 2018 May 02; 140(17): 5842–5852. doi:10.1021/jacs.8b02658.

Controlling the oligomerization state of Aβ-derived peptides with light

Patrick J. Salveson, **Sepehr Haerianardakani**, **Alexander Thuy-Boun**, **Adam G. Kreutzer**, and **James S. Nowick***

Department of Chemistry, University of California, Irvine, Irvine, CA, 92697-2025, United States

Abstract

A key challenge in studying the biological and biophysical properties of amyloid-forming peptides is that they assemble to form heterogenous mixtures of soluble oligomers and insoluble fibrils. Photolabile protecting groups have emerged as tools to control the properties of biomolecules with light. Blocking intermolecular hydrogen bonds that stabilize amyloid oligomers provides a general strategy to control the biological and biophysical properties of amyloid-forming peptides. This paper describes the design, synthesis, and characterization of macrocyclic β-hairpin peptides that are derived from amyloidogenic peptides and contain the *N*-2-nitrobenzyl photolabile protecting group. Each peptide contains two heptapeptide segments from $A\beta_{16–36}$ or $A\beta_{17–36}$ constrained into β-hairpins. The *N*-2-nitrobenzyl group is appended to the amide backbone of Gly_{33} to disrupt the oligomerization of the peptides by disrupting intermolecular hydrogen bonds. X-ray crystallography reveals that *N*-2-nitrobenzyl groups can either block assembly into discrete oligomers or permit formation of trimers, hexamers, and dodecamers. Photolysis of the *N*-2-nitrobenzyl groups with long-wave UV light unmasks the amide backbone and alters the assembly and the biological properties of the macrocyclic β-hairpin peptides. SDS-PAGE studies show that removing the *N*-2-nitrobenzyl groups alters the assembly of the peptides. MTT conversion and LDH release assays show that decaging the peptides induces cytotoxicity. Circular dichroism studies and dye leakage assays with liposomes reveal that decaging modulates interactions of the peptides with lipid bilayers. Collectively, these studies demonstrate that incorporating *N*-2-nitrobenzyl groups into macrocyclic β-hairpin peptides provides a new strategy to probe the structures and the biological properties of amyloid oligomers.

Graphical Abstract

*Corresponding Author James S. Nowick jsnowick@uci.edu, Phone: (949) 824-6091.

Supporting Information Available

Procedures for the synthesis of peptides **1**–**4**, as well as trimers **3** and **4**; details of the crystallization, X-ray diffraction data collection, processing, and refinement of peptide $\mathbf{1^{I}_{NB}}$ and trimer **3**; procedures for photolysis of *N*-2-nitrobenzyl protected peptides, cell culture, MTT and LDH assays, liposome preparation and dye leakage assays, circular dichroism spectroscopy, and SDS-PAGE; crystallographic data in CIF format. Crystallographic coordinates of peptide $\mathbf{1^{I}_{NB}}$ and trimer 3 were deposited into the Protein Data Bank with PDB codes 6CG3, 6CG4 and 6CG5.

This material is available free of charge via the Internet at http://pubs.acs.org/.

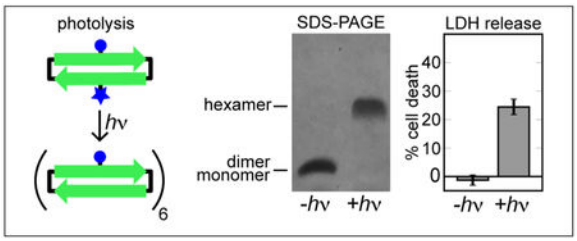

Introduction

Photolabile protecting groups have enabled the control of myriad biological properties by allowing the release of biologically active molecules at precise times and locations.[1–4] These protecting groups have revealed hitherto unknown biology through the precise control afforded by light. Photocaged neurotransmitters have enabled the selective activation of signaling pathways in subpopulations of neurons.[5–7] The control gained using photolabile protecting groups has been leveraged in other applications, including protein dimerization, immune cell activation, transcription, and hydrogel formation.[8–19] Expanding the control afforded by photolabile protecting groups to oligomers of Aβ may help dissect the biological properties of these enigmatic species associated with Alzheimer's disease.

Soluble oligomers of Aβ are closely associated with neurodegeneration in Alzheimer's disease. The oligomers are heterogeneous and polymorphic, ranging in size from dimers, trimers, and dodecamers to large annular protofibrils weighing 100–150 kDa.[20] The large Aβ oligomers are thought to comprise multiple copies of smaller oligomers, further complicating the Aβ oligomer landscape. A putative Aβ dodecamer, termed Aβ*56, is thought to comprise multiple trimeric subunits of Aβ.[21] Annular protofibrils have been proposed to comprise multiple hexameric assemblies of Aβ.[22] These differently sized Aβ oligomers, prepared or isolated in different fashions, have different biological properties such as cytotoxicity, synaptotoxicity, and membrane permiabilization.[23,24] The structural heterogeneity of Aβ oligomers renders them intractable to high-resolution structural characterization by X-ray crystallography or NMR spectroscopy. Methods that limit the structural heterogeneity of Aβ oligomers enable the dissection of their structures and biological properties. Thus far, studies of photocaged amyloid-forming peptides and proteins have focused on controlling the aggregation and disaggregation of fibrils.[25–28] To our knowledge, photocaged amyloid-forming peptides have not been used to study amyloid oligomers.

Chemical model systems derived from amyloidogenic peptides and proteins are attractive for exploring the ability of photolabile protecting groups to control the formation of amyloid oligomers. Chemical model systems can limit the structural heterogeneity of amyloid oligomers and provide insights into the assemblies and the biology of amyloid-forming proteins, including Aβ.[29–36] Through the use of chemical model systems, researchers have elucidated the principles that govern the assembly of amyloidogenic peptides and proteins. Eisenberg and coworkers, for example, have observed the formation of "steric zippers" that stabilize amyloid fibrils.[37,38] These steric zippers have guided the structure-based design of

molecules capable of blocking steric zipper formation, and thus preventing aggregation of full-length amyloidogenic peptides and proteins.[39,40]

Our research group has developed chemical model systems that provide insights into the structures and assembly of Aβ oligomers. [30,32–35] These model systems are based on macrocyclic β-hairpins derived from Aβ. β-Hairpins have emerged as key building blocks of Aβ oligomers.[22,41–47] We have crystallized a number of these macrocyclic β-hairpins and elucidated their structures through X-ray crystallography. The X-ray crystallographic structures have revealed a hierarchical assembly of the macrocyclic β-hairpins into oligomers. These structures have led us to propose models in which Aβ folds into β-hairpins that assemble into triangular trimers and related higher-order oligomers.[32,48]

The chemical model systems that our laboratory has developed to study the oligomerization of Aβ-derived peptides contain two heptapeptide β-strands from Aβ connected by two δ-linked ornithine ($^{\delta}$Orn) β-turn mimics.[49] These macrocyclic β-hairpin peptides contain *N*-methyl groups, which limit the uncontrolled aggregation of the hydrophobic peptides.[50] Our laboratory recently reported β-hairpin peptides **1** and **2**, which are designed to mimic β-hairpins adopted by $A\beta_{17–36}$ and $A\beta_{16–36}$ (Chart 1).[30,35] Both peptides **1** and **2** contain the heptapeptide β-strand $A\beta_{30–36}$. In peptide **1**, the $A\beta_{30–36}$ β-strand is juxtaposed with $A\beta_{17–23}$; in peptide **2**, the $A\beta_{30–36}$ β-strand is juxtaposed with $A\beta_{16–22}$. Both peptides bear a single *N*-methyl group. The *N*-methyl group is on Gly_{33} in peptide **1**, and on Phe_{19} in peptide **2**. Peptides **1** and **2** assemble in different fashions. Peptide **1** assembles to form triangular trimers, which further assemble to form ball-shaped dodecamers and sandwich-like hexamers.[30] Peptide **2** assembles to form a compact hexamer.[35] Photoprotected homologues of peptides **1** and **2** may allow their assembly and biological properties to be controlled.

In the current paper, we set out to explore the use of light to switch the oligomerization state of β-hairpin peptides derived from Aβ. Our laboratory has previously observed that extensive intermolecular hydrogen-bonding networks stabilize the oligomers formed by both peptides **1** and **2**. In this study, we hypothesized that photolabile protecting groups installed at locations designed to disrupt these hydrogen-bonding networks would allow the assembly of the peptides to be controlled. We began by determining whether replacing the *N*-methyl group of peptide **1** with an *N*-2-nitrobenzyl group would limit aggregation while not altering the assembly into triangular trimers (Figure 1A). We then asked if we could apply the *N*-2-nitrobenzyl group to switch on the toxicity of peptide **2** by controlling its oligomerization state (Figure 1B). Finally, we applied the *N*-2-nitrobenzyl group to trimeric homologues of peptide **1**, which assemble to form hexamers or dodecamers depending on the location of the *N*-methyl group (Figure 1C). Collectively, these experiments reveal that homologues of peptides **1** and **2** containing *N*-2-nitrobenzyl groups can readily be prepared and that their photolysis enables the assembly and the biological properties of the peptides to be controlled with light.

Results and Discussion

The following three sections describe and expand upon the experiments outlined in Figure 1A, B, and C. In the first set of experiments, we develop a synthetic method to incorporate *N*-2-nitrobenzyl groups into macrocyclic β-hairpin peptides, characterize their assemblies by X-ray crystallography, and demonstrate that we can remove the *N*-2-nitrobenzyl groups with long-wave UV light. In the second set of experiments, we expand on the results from the first set by using the *N*-2-nitrobenzyl group and light to control both the assembly and the biological properties of peptide **2**. In the final set of experiments, we expand upon the findings from the first two sets of experiments, by preparing a covalently crosslinked trimer derived from peptide $\mathbf{1_{NB}}$ and altering its assembly with light.

1. Developing Macrocyclic β-Hairpin Peptides that Contain an *N*-2-nitrobenzyl Group.

To test whether the *N*-2-nitrobenzyl group would limit uncontrolled assembly of macrocyclic β-hairpin peptides in the same fashion as an *N*-methyl group, we prepared and studied peptide $\mathbf{1_{nb}}$, a homologue of peptide **1** (Chart 2). We hypothesized that an *N*-2-nitrobenzyl group would be tolerated by the triangular trimer formed by peptide **1**, while also limiting the aggregation of the photocaged peptide in the same fashion as an *N*-methyl group (Figure 2). We prepared peptide $\mathbf{1_{NB}}$ and characterized its assembly by X-ray crystallography to ascertain the effect of replacing the *N*-methyl group with an *N*-2-nitrobenzyl group.

Synthesis.—We synthesized peptide $\mathbf{1_{NB}}$ using solid-phase Fmoc-based peptide synthesis followed by solution-phase macrocyclization. *N*-2-nitrobenzylglycine$_{33}$ was not introduced as an Fmoc-protected amino acid, but rather constructed using a submonomer approach, wherein the growing peptide was acylated with bromoacetic acid, and the α-bromo group as then displaced with 2-nitrobenzylamine (Scheme S2).[28,51] Subsequent coupling of Ile$_{32}$ to *N*-2-nitrobenzylglycine$_{33}$ proved far more difficult than coupling to *N*-methylglycine$_{33}$ (Figure S1). Using HATU and HOAt to activate Fmoc-Ile$_{32}$-OH resulted in multiple products. In contrast, using triphosgene to activate Fmoc-Ile$_{32}$-OH as the acid chloride afforded the Ile$_{32}$-coupled peptide as the single product.[52] Four 1-hour couplings using triphosgene gave 95% conversion to the Ile$_{32}$-coupled product, whereas four 6-hour couplings using HATU and HOAt to activate Fmoc-Ile$_{32}$-OH resulted in little (< 20%) coupling. Triphosgene facilitates this difficult amidation and enables the preparation of 10–30 mg of peptide $\mathbf{1_{NB}}$ from a 0.1-mmol scale synthesis.[53] We incorporated 4-iodophenylalanine (Phe^{I}) in place of Phe$_{19}$ in peptide $\mathbf{1^{I}_{NB}}$ to facilitate X-ray crystallographic phase determination using single-wavelength anomalous diffraction phasing.[54]

X-ray crystallography.—Peptide $\mathbf{1^{I}_{NB}}$ crystalizes in similar conditions as peptide **1**:[55] 0.1 M HEPES, buffered at pH 8.75, supplemented with 18% (w/v) Jeffamine M-600.[56] Diffraction data were collected to 2.03 Å. The structure of peptide $\mathbf{1^{I}_{NB}}$ was solved and refined in space group P4$_2$32. The asymmetric unit contains a single copy of peptide $\mathbf{1^{I}_{NB}}$ folded into a β-hairpin (Figure 3A). The *N*-2-nitrobenzyl group is clearly visible in the

electron density map (Figure S2). Table S1 summarizes the crystallographic properties, crystallization conditions, data collection, and model refinement statistics for peptide $\mathbf{1^{I}_{NB}}$.

Peptide $\mathbf{1^{I}_{NB}}$ assembles in an identical fashion to peptide **1** and several related homologues that our laboratory has previously reported. [30,32,34] The single copy of peptide $\mathbf{1^{I}_{NB}}$ within the asymmetric unit is folded into a β-hairpin; three copies of peptide $\mathbf{1^{I}_{NB}}$ occupy the edges of an equilateral triangle (Figure 3B); four copies of this trimer assemble in a tetrahedral fashion to form a ball-shaped dodecamer (Figure S3); the interface between dodecamers constitutes a sandwich-like hexamer (Figure 3C). The lattice readily accommodates the *N*-2-nitrobenzyl group without substantial changes in structure or assembly, with the *N*-2-nitrobenzyl group from one trimer packing against the side chains of $^{\delta}Orn_2$ and Glu_{22} from a separate trimer within the sandwich-like hexamer. Thus, the *N*-2-nitrobenzyl group does not prevent peptide $\mathbf{1^{I}_{NB}}$ from forming triangular trimers and related higher-order oligomers.

The assembly of peptide $\mathbf{1^{I}_{NB}}$ into trimers, hexamers, and dodecamers highlights the proclivity of $A\beta_{17–36}$ to form triangular trimers when it is constrained into a β-hairpin. Replacing the *N*-methyl group in peptide **1** with an *N*-2-nitrobenzyl group does not alter the assembly of the peptide. Our research group has previously observed that a homologue of peptide **1** containing the $A\beta_{24–29}$ loop also assembles into trimers, hexamers, and dodecamers.[32] Thus, the triangular trimer tolerates substantial modifications and the incorporation of additional residues from Aβ. The formation of triangular trimers appears to be an innate property of β-hairpins encompassing $A\beta_{17–36}$.

Photodecaging.—We evaluated the photolysis of peptide $\mathbf{1_{NB}}$ using a hand-held long-wave (365 nm) UV lamp. We monitored the photolysis of a 2 mg/mL solution of peptide $\mathbf{1_{NB}}$ in a 1 cm quartz cuvette by both RP-HPLC and mass spectrometry (Figure 4). Under these conditions, the decaging appears to follow first-order kinetics, reaching approximately 50% completion in 10 minutes. Irradiation of peptide $\mathbf{1_{NB}}$ for 1 hour results in the complete photolysis of the *N*-2-nitrobenzyl group. In these studies, we found that the 2-nitrosobenzaldehyde by-product reacts with amine groups of peptide $\mathbf{1_{NB}}$. Addition of cysteine to scavenge this by-product eliminates this side reaction.[52]

The synthetic, X-ray crystallographic, and photolytic studies of peptides $\mathbf{1_{NB}}$ and $\mathbf{1^{I}_{NB}}$ establish that the *N*-2-nitrobenzyl group can readily be incorporated into macrocyclic β-hairpin peptides and that it can be removed with light. These studies set the stage for applying the *N*-2-nitrobenzyl group to control the assembly and the biological properties of other macrocyclic β-hairpins.

2. Controlling the Biological Properties of a Macrocyclic β-Hairpin Peptide with Light.

We next sought to apply the *N*-2-nitrobenzyl group to control the formation of toxic oligomers of a macrocyclic β-hairpin peptide. Our research group has previously shown that peptide **2** is toxic towards the neuroblastoma cell-line SH-SY5Y, and that it assembles to form a hexamer, which is observed crystallographically and in SDS-PAGE.[35] The hexamer cannot accommodate *N*-alkylation of Gly_{33}, which hydrogen bonds with Ile_{31} (Figure 5). We hypothesized that replacing Gly_{33} with *N*-2-nitrobenzylglycine would disrupt hydrogen bonding and thus disrupt assembly of the toxic hexamer. Photolysis of the *N*-2-nitrobenzyl

group would uncage Gly_{33} and allow the hexamer to assemble, thereby switching on the biological properties of the peptide. We synthesized peptide $\mathbf{2_{NB}}$ using the submonomer approach described in the preceding section. We studied its assembly in SDS-PAGE, its cytotoxicity, and its interactions with lipid bilayers to test if the *N*-2-nitrobenzyl group can control both the assembly and the biological properties of a macrocyclic β-hairpin peptide (Chart 3).

SDS-PAGE.—Unlike peptide **2**, peptide $\mathbf{2_{NB}}$ does not assemble to form a hexamer in SDS-PAGE (Figure 6). To ascertain the impact of *N*-alkylation of Gly_{33}, we compared the assembly of peptide **2** to that of peptide $\mathbf{2_{NB}}$ and peptide $\mathbf{2_{Me}}$, a homologue bearing an additional *N*-methyl group, on Gly_{33}. In tricine SDS-PAGE, peptide **2** migrates with a similar mobility to the 10 kDa size standard. This mobility is consistent with peptide **2** assembling to form a hexamer (10.6 kDa). In contrast, peptides $\mathbf{2_{Me}}$ and $\mathbf{2_{NB}}$ migrate between the 1.7 and the 4.6 kDa size standards and thus appear to be monomers or dimers. The mobility of peptide $\mathbf{2_{NB}}$ shifts after photodecaging with a hand-held UV lamp. The resulting band migrates with a mobility similar to that of peptide **2**. Thus, the *N*-2-nitrobenzyl group and its photolysis allows the oligomerization state of peptide **2** to be controlled with light.

Cytotoxicity.—In addition to altering the assembly of the hexamer, *N*-2-nitrobenzylation alters the biological properties of peptide **2**. Peptide $\mathbf{2_{NB}}$ is not toxic at concentrations as high as 100 μM as measured by both LDH release and MTT conversion assays against the neuroblastoma cell-line SH-SY5Y (Figure 7 and S4). In contrast, peptide **2** is toxic at concentrations as low as 50 μM. Irradiating peptide $\mathbf{2_{NB}}$ with long-wave UV light switches on the toxicity of the peptide. This toxicity results from the formation of peptide **2** and not from the formation of the nitrosobenzaldehyde by-product, as the photolysis of peptide $\mathbf{1_{NB}}$ does not result in toxicity.

Interactions with liposomes.—To evaluate whether the toxicity of peptide **2** arrises from its disruption of cell membranes, we studied the effect of peptide **2** on liposomes using a dye leakage assay. In this assay, large unilamellar vesicles (LUVs) encapsulating the fluorescent dye calcein were treated with peptide **2** and the increase in fluorescence was monitored. Peptide **2** induces anionic LUVs to leak their contents (Figure 8). Peptide **2** induces measurable dye leakage from LUVs composed of a 1:1 mixture of phosphatidylcholine and phosphatidylserine (PC:PS) at concentrations as low as *ca*. 300 nM. Peptide **2** induces 50% dye leakage at *ca*. 2 μM. In contrast, peptide $\mathbf{2_{NB}}$ induces comparable leakage at 20 μM. The contrasting activities of peptide **2** and peptide $\mathbf{2_{NB}}$ in dye leakage assays indicate that caging peptide **2** with the *N*-2-nitrobenzyl group reduces its ability to disrupt membranes. The roughly ten-fold difference in membrane disrupting activity between peptide **2** and peptide $\mathbf{2_{NB}}$ parallels the greater toxicity of peptide **2** over peptide $\mathbf{2_{NB}}$ described above.

Both peptides **2** and $\mathbf{2_{NB}}$ are substantially less active towards neutral LUVs composed of only phosphatidylcholine (Figure 8). Peptide **2** induces *ca*. 33% dye leakage at 20 μM (the highest concentration tested), whereas peptide $\mathbf{2_{NB}}$ does not induce any measurable dye

leakage from PC LUVs. The contrasting behavior of PC:PS LUVs and PC LUVs indicates that electrostatic interactions between the cationic peptides and the anionic liposomes are essential to the dye leakage activity of peptide **2**.

Irradiation of peptide $\mathbf{2_{NB}}$ with long-wave UV light in the presence of PC:PS LUVs restores the dye leakage activity (Figure 9). Photolysis of peptide $\mathbf{2_{NB}}$ appears to proceed at a similar rate to the photolysis of peptide $\mathbf{1_{NB}}$. Irradiating 5 μM peptide $\mathbf{2_{NB}}$ for 10 minutes results in an increase in dye leakage from PC:PS LUVs. Irradiating peptide $\mathbf{2_{NB}}$ for 1 hour restores nearly all of the activity that results from treatment with an equal concentration of peptide **2**. Thus, the *N*-2-nitrobenzyl group and its photolysis allows the membrane disrupting activity of peptide **2** to be controlled with light.

To evaluate the effect of membranes on the conformations of peptides **2** and $\mathbf{2_{NB}}$, we compared the CD spectra of the peptides in aqueous buffer to those of the peptides in the presence of either anionic (PC:PS) or neutral (PC) liposomes (Figure 10). The CD spectrum of peptide **2** in buffer displays a broad minimum from 207 nm to 216 nm. This spectrum does not appear to be consistent with predominance of either β-sheets or random coils.[57] Upon mixing peptide **2** with anionic liposomes, the minimum sharpens and shifts to 218 nm. In contrast, neutral LUVs have little effect on the CD spectrum. This change in the CD spectrum suggests that interacting with anionic lipids, but not neutral lipids, induces β-sheet folding in peptide **2**. These differing effects of PC and PC:PS LUVs on membrane-induced folding are congruent with the role of electrostatic interactions in the dye leakage assays.

Similar conformational changes are observed when peptide $\mathbf{2_{NB}}$ is mixed with anionic liposomes. The CD spectra of peptide $\mathbf{2_{NB}}$ in buffer and in the presence of neutral liposomes display minima at *ca.* 205 nm. Upon mixing peptide $\mathbf{2_{NB}}$ with anionic liposomes, the minimum shifts to *ca.* 218 nm. These studies with liposomes support a model in which the *N*-2-nitrobenzyl group does not prevent peptide $\mathbf{2_{NB}}$ from interacting with anionic lipids but instead prevents the formation of oligomers that cause dye leakage.

The SDS-PAGE, cytotoxicity, and liposome studies establish that the *N*-2-nitrobenzyl group can be incorporated into macrocyclic peptides to control both their assembly and their biological properties. The *N*-2-nitrobenzyl group in peptide $\mathbf{2_{NB}}$ disrupts its assembly into hexamers in SDS-PAGE, markedly reduces its toxicity, and decreases its ability to induce membrane leakage. Removal of the *N*-2-nitrobenzyl group with long-wave UV light restores hexamer formation, toxicity, and membrane leakage. Collectively these studies suggest that peptide **2** is toxic to SH-SY5Y cells through a mechanism that involves membrane disruption, mediated by oligomers of the peptide.

3. Controlling the Assembly of Triangular Trimers with Light.

The ability of the *N*-2-nitrobenzyl group to control the assembly of peptide **2** suggested that we could incorporate *N*-2-nitrobenzyl groups into a covalently crosslinked trimer derived from peptide $\mathbf{1_{NB}}$. Our laboratory has previously developed two crosslinked trimeric homologues of peptide **1** to gain insights into the biological properties of the triangular trimer motif (Figure 11A).[33] These trimers are identical in amino acid sequence and only differ in the placement of three *N*-methyl groups. The *N*-methyl groups are on Gly_{33} in

trimer **1**, blocking the $A\beta_{30–36}$ β-strands from further hydrogen bonding, while the *N*-methyl groups are on Phe_{20} in trimer **2**, allowing the $A\beta_{30–36}$ β-strands to further hydrogen bond. Trimers **1** and **2** assemble to form different oligomers due to blocking or exposing the $A\beta_{30–36}$ β-strands. Trimer **1** assembles as a hexamer, which is observed crystallographically and in SDS-PAGE; trimer **2** assembles as a dodecamer, which is also observed crystallographically and in SDS-PAGE. Gly_{33} participates in a hydrogen-bonding interface with Ile_{31} within the dodecamer (Figure 11B). We hypothesized that replacing the *N*-methyl groups in trimer **1** with photolabile *N*-2-nitrobenzyl groups would result in a triangular trimer that forms a hexamer and that photolysis of the *N*-2-nitrobenzyl groups would switch the supramolecular assembly to a dodecamer (Figure 11C). To test this hypothesis, we prepared and studied photocaged trimer **3**, which contains three *N*-2-nitrobenzyl groups.

Synthesis.—The X-ray crystallographic structure of peptide $\mathbf{1^{I}_{NB}}$ suggests a strategy for forming a covalently crosslinked trimer and testing the ability of the *N*-2-nitrobenzyl group to control assembly. At the three vertices of the triangular trimer, depicted in Figure 3B, the side chains of Leu_{17} and Ala_{21} pack against one another. Mutation of these two residues to Cys permits the formation of the *tris*-disulfide crosslinked photocaged trimer **3**, in an analogous fashion to the formation of trimers **1** and **2** that our laboratory has previously reported.[33] With the goal of forming trimer **3**, we prepared peptide $\mathbf{3_{NB}}$, which bears the L17C and A21C mutations (Chart 4).

Oxidation of peptide $\mathbf{3_{NB}}$ with 20% aqueous DMSO produces three species: a *tris*-disulfide crosslinked trimer, a *bis*-disulfide crosslinked dimer, and a monomer containing an intramolecular disulfide bond (Figure 12).[58,59] The identities of the trimer, dimer, and monomer were established by examining the isotope patterns of the multiply charged ions in the electrospray ionization mass spectrum. We purified trimer **3** using RP-HPLC followed by lyophilization of pure fractions. From the oxidation of *ca.* 60 mg of peptide $\mathbf{3_{NB}}$, we were able to prepare 14 mg of trimer **3** (*ca.* 23% yield). Photolysis of trimer **3** for two hours with long-wave UV light readily affords deprotected trimer **4**. As with the photolysis of peptide $\mathbf{1_{NB}}$, cysteine is added to the photolysis reaction to scavenge the nitrosobenzaldehyde by-product. [52] We purified trimer **4** using RP-HPLC followed by lyophilization of pure fractions. From the photolysis of 10 mg of trimer **3**, we were able to isolate 5 mg of trimer **4** (*ca.* 50% yield).

It is not possible to prepare trimer **4** by directly oxidizing peptide **4** (Chart 4). Peptide **4**, which contains neither an *N*-methyl group nor an *N*-2-nitrobenzyl group, does not form a crosslinked trimer upon oxidation in aqueous DMSO. Instead, peptide **4** only forms a disulfide monomer (Figures 13 and S5). The *N*-2-nitrobenzyl group enables the synthesis of trimer **4** by acting as a traceless aggregation-blocking group that can be removed with light.

SDS-PAGE.—The *N*-2-nitrobenzyl group serves as a switch that alters the supramolecular assembly of the triangular trimer motif upon photolysis and liberation of the $A\beta_{30–36}$ β-strands (Figure 14). Trimer **1** and photocaged trimer **3** contain blocked $A\beta_{30–36}$ β-strands and migrate in SDS-PAGE at similar mobilities to the 10 kDa size standard. These mobilities are consistent with trimer **1** and trimer **3** assembling to form hexamers (10.6 and 11.3 kDa).

In contrast, trimer **2** and trimer **4** contain exposed $A\beta_{30–36}$ β-strands and migrate in SDS-PAGE between the 17 and 26 kDa size standards. These mobilities are consistent with trimer **2** and trimer **4** assembling to form dodecamers (21.2 and 21.0 kDa). Both dodecamer bands show pronounced downward streaking, indicating an equilibrium with smaller oligomers, such as hexamers or nonamers. In contrast, peptide $\mathbf{1_{NB}}$ does not assemble into higher-order oligomers and instead migrates between the 1.7 and 4.6 kDa size standards and thus appears to be a monomer or a dimer.

X-ray crystallography.—We turned to X-ray crystallography to gain insights into the assembly of trimers **3** and **4** into the hexamers and dodecamers observed in SDS-PAGE. Trimer **3** does not grow crystals in similar conditions as either trimer **1** or trimer **2**. Instead, trimer **3** crystalizes from a mixture of 0.1 M sodium acetate, buffered at pH 4.5, 0.2 M NaCl, and 28% (w/v) 2-methyl-2,4-pentanediol. We determined the X-ray crystallographic phases by soaking a crystal for 1 hour in a mixture of 0.1 M potassium iodide (KI) and crystallization buffer. We used the program BLEND to merge multiple data sets from a single crystal and found that doing so allowed single-wavelength anomalous diffraction phasing.[60] The X-ray crystallographic structure of the KI-soaked trimer **3** (PDB 6CG4) was then used as a search model in molecular replacement to determine the X-ray crystallographic phases of a data set collected from a crystal that had not been soaked in KI (PDB 6CG5). Both structures of trimer **3** were solved and refined in space group $I4_1$ at 2.03 Å resolution. Table S1 summarizes the crystallographic properties, crystallization conditions, data collection, and model refinement statistics.

Trimer **4** does not grow crystals in similar conditions as trimers **1**–**3**. Screening trimer **4** in 288 conditions yielded a single condition in which crystals grow: a mixture of 0.1 M HEPES, buffered at pH 7.25, and 20% (v/v) Jeffamine M-600.[61] Unfortunately, our attempts to optimize these conditions have thus far only yielded crystals that diffract X-rays weakly. We have been unable to process the resulting data sets and thus have been unable to solve the X-ray crystallographic structure of trimer **4**.

The crystals of trimer **3** contain a single copy of trimer **3** in the asymmetric unit (Figure 15A). The X-ray crystallographic structure of trimer **3** reveals a symmetrical trimer composed of three folded β-hairpins. The trimer is stabilized by three disulfide bonds wherein Cys_{17} of one monomer is linked to Cys_{21} of another monomer at the three vertices of the triangular trimer. The *N*-2-nitrobenzyl groups pack against the Phe_{20} side chains on the bottom surface of trimer **3** (Figure 15B). The three *N*-2-nitrobenzyl groups are clearly visible in the electron density map (Figure S6). The *N*-2-nitrobenzyl groups also make intermolecular contacts with neighboring trimers in the crystal lattice, packing against the $^{\delta}Orn_1$ turns from other trimers and interacting with other *N*-2-nitrobenzyl groups. Unlike the discrete oligomers formed by trimers **1** and **2**, no discrete oligomers exist in the crystal lattice formed by trimer **3**.

The assembly of trimer **3** in the crystal lattice differs from the assemblies of trimers **1** and **2**. Trimer **1** assembles into stacks of sandwich-like hexamers, which resemble the sandwich-like hexamer formed by peptide $\mathbf{1^I_{NB}}$ (Figure S7A). Trimer **2** assembles into ballshaped dodecamers (Figure S7B). We anticipated that trimer **3** would assemble in a similar fashion

to trimer **1**, as the $A\beta_{30–36}$ β-strands in both trimers are blocked from hydrogen bonding. Instead, trimer **3** assembles into conjoined dodecamers in which each trimer subunit is shared between two dodecamers in the crystal lattice. These conjoined dodecamers do not resemble the dodecamers formed by trimer **2**. The dodecamers formed by trimer **3** assemble through heterofacial packing of the composite trimer subunits. In contrast, the dodecamers formed by trimer **2** assemble through homofacial packing of the composite trimer subunits. Sequestration of the *N*-methyl groups within trimer **2**3 exposes the $A\beta_{30–36}$ β-strands to further hydrogen-bonding interactions within the trimer **2** dodecamer. The *N*-2-nitrobenzyl groups in trimer **3** do not permit this mode of hydrogen bonding. As a result, the hydrogen-bonding network in the trimer **2** dodecamer is more extensive than that in the trimer **3** dodecamer.

The X-ray crystallographic structure of the conjoined dodecamers formed by trimer **3** offers little insight into the hexamers that it forms in SDS-PAGE, because these dodecamers do not contain discrete hexamer subunits. The sandwich-like hexamers formed by trimer **1** (PDB 5SUT), on the other hand, support a working model for the structures of these hexamers. In this working model, two trimers sandwich together. Such a model is consistent with other sandwich-like hexamers we have observed in the crystal lattices of other macrocyclic β-hairpin peptides. [30,32–34,62]

We have not been able to determine the X-ray crystallographic structure of trimer **4** and thus lack a structure to help illuminate the dodecamers it forms in SDS-PAGE. The ball-shaped dodecamers formed by trimer **2** (PDB 5SUR) provide a working model for these dodecamers. In this working model, four trimers wrap together to form a ball. Such a model is consistent with other ball-shaped dodecamers we have observed in the crystal lattices of other macrocyclic β-hairpin peptides.[34] Such a model is also consistent with the differing oligomerization states observed for trimers **3** and **4** in SDS-PAGE.

The synthetic, SDS-PAGE, and X-ray crystallographic studies of trimers **3** and **4** establish that the *N*-2-nitrobenzyl group is sufficiently robust to be incorporated into covalently crosslinked oligomers containing multiple peptides and *N*-2-nitrobenzyl groups. These studies further establish that the *N*-2-nitrobenzyl group can allow light to switch the peptide from one oligomerization state to another.

Conclusion

The *N*-2-nitrobenzyl photolabile protecting group allows the oligomerization state of Aβ-derived macrocyclic peptides to be controlled with light. Depending on their positions, the *N*-2-nitrobenzyl groups can either be accommodated by or disrupt the higher-order assemblies of the macrocyclic peptides. Disrupting intermolecular hydrogen bonds that stabilize the oligomers observed by X-ray crystallography disrupts the assembly of the peptides in solution. Their assembly can be recovered by irradiating the peptides with long-wave UV light, which removes the *N*-2-nitrobenzyl groups. In the case of peptide $\mathbf{2_{NB}}$, the *N*-2-nitrobenzyl group also alters the biological properties of the peptide. Removing the *N*-2-nitrobenzyl group from peptide $\mathbf{2_{NB}}$ restores both the assembly and the biological properties of peptide **2**. The *N*-2-nitrobenzyl group offers the promise of controlling when

and where macrocyclic β-hairpin peptides assemble in cells. In the case of trimer **3**, the *N*-2-nitrobenzyl group enables the synthesis of trimer **4**, which lacks any *N*-alkyl groups. Trimer **4** should better model the types of trimers that full-length Aβ may form and thus allow us to better probe the biology of Aβ oligomers.

We envision that *N*-2-nitrobenzyl groups could be applied to chemical model systems of other amyloid oligomers. The αB crystallin-derived cylindrin oligomers and the SOD1-derived corkscrew oligomers reported by Eisenberg and co-workers, as well as the hPrP-dervied hexameric oligomers reported by Surewicz and co-workers, are all amenable to the strategy described here. [29,36,63] Controlling the assembly of these chemical model systems may enable the biological properties of these oligomers to be probed. The aforementioned structures may even guide the installation of photolabile protecting groups into full-length amyloid-forming peptides and proteins. We envision that the *N*-2-nitrobenzyl group will enable a more rigorous dissection of the relationship between the assembly and the biological properties of amyloid-derived peptides. Studies in this direction are currently underway in our laboratory.

Supplementary Material

Refer to Web version on PubMed Central for supplementary material.

Acknowledgement

This work was supported by the National Institutes of Health (GM097562). The authors thank the Laser Spectroscopy Facility at University of California, Irvine for assistance with circular dichroism measurements. P.J.S. thanks the UCI Training Program in Chemical and Structural Biology for training grant support (T32 GM108561) as well as ARCS Foundation Orange County for additional support.

Notes and References

(1). Young DD; Deiters A Photochemical control of biological processes. Org. Biomol. Chem. 2007, 5, 999–1005. [PubMed: 17377650]

(2). Yu H; Li J; Wu D; Qiu Z; Zhang Y Chemistry and biological applications of photo-labile organic molecules. Chem. Soc. Rev 2010, 39, 464–473. [PubMed: 20111771]

(3). Klán R; Šolomek T; Bochet CG; Blanc A; Givens R; Rubina M; Popik V; Kostikov A; Wirz J Photoremovable protecting groups in chemistry and biology: reaction mechanisms and efficacy. Chem. Rev 2012, 113, 119–191. [PubMed: 23256727]

(4). Ankenbruck N; Courtney T; Naro Y; Deiters A Optochemical control of biological processes in cells and animals. Angew. Chem. Int. Ed 2018, 57, 2–33.

(5). Callaway EM; Yuste R Stimulating neurons with light. Curr. Opin. Neurobiol 2002, 12, 587–592. [PubMed: 12367640]

(6). Kramer RH; Chambers JJ; Trauner D Photochemical tools for remote control of ion channels in excitable cells. Nat. Chem. Biol 2005, 1, 360–365. [PubMed: 16370371]

(7). Ellis-Davies GCR Neurobiology with caged calcium. Chem. Rev 2008, 108, 1603–1613. [PubMed: 18447376]

(8). Haines LA; Rajagopal K; Obzas B; Salick DA; Pochan DJ; Schneider JP Light-activated hydrogel formation via the triggered folding and self-assembly of a designed peptide. J. Am. Chem. Soc 2005, 127, 17025–17029. [PubMed: 16316249]

(9). Karginov AV; Zou Y; Shirvanyants D; Kota P; Dokholyan NV; Young DD; Hahn KM; Deiters A Light regulation of protein dimerization and kinase activity in living cells using photocaged rapamycin and engineered FKBP. J. Am. Chem. Soc 2011, 133, 420–423. [PubMed: 21162531]

(10). Umeda N; Neno T; Pohlmeyer C; Nagano T; Inoue T A photocleavable rapamycin conjugate for spatiotemporal control of small GTPase activity. J. Am. Chem. Soc 2011, 133, 12–14. [PubMed: 21142151]

(11). Deiters A Light activation as a method of regulating and studying gene expression. Curr. Opin. Chem. Biol 2009, 13, 678–686. [PubMed: 19857985]

(12). Govan JM; Lively MO; Deiters A Photochemical control of DNA decoy function enables precise regulation of nuclear factor κB activity. J. Am. Chem. Soc 2011, 133, 13176–13182. [PubMed: 21761875]

(13). Ryu KA; Stutts L; Tom JK; Mancini RJ; Esser-Kahn AP Stimulation of innate immune cells by light-activated TLR7/8 agonists. J. Am. Chem. Soc 2014, 136, 10823–10825. [PubMed: 25029205]

(14). Mancini RJ; Stutts L; Moore T; Esser-Kahn AP Controlling the origins of inflammation with a photoactive lipopeptide immunopotentiator. Angew. Chem. Int. Ed 2015, 54, 5962–5965.

(15). Stutts L; Esser-Kahn AP A light-controlled TLR4 agonist and selectable activation of cell subpopulations. Chembiochem 2015, 16, 1744–1748. [PubMed: 26097006]

(16). Schelkle KM; Griesbaum T; Ollech D; Becht S; Buckup T; Hamburger M; Wombacher R Light-induced protein dimerization by one- and two-photon activation of gibberellic acid derivatives in living cells. Angew. Chem. Int. Ed 2015, 54, 2825–2829.

(17). Brown KA; Zou Y; Shirvanyants D; Zhang J; Samanta S; Mantravadi PK; Dokholyan NV; Deiters A Light-cleavable rapamycin dimer as an optical trigger for protein dimerization. Chem. Commun 2015, 51, 5702–5705.

(18). Smith DJ; Brat GA; Medina SH; Tong D; Huang Y; Grahammer J; Furtmüller GJ; Oh BC; Nagy-Smith KJ; Walczak P; Brandacher G; Schneider JP A multiphase transitioning peptide hydrogel for suturing ultrasmall vessels. Nat. Nanotechnol 2016, 11, 95–102. [PubMed: 26524396]

(19). Ryu KA; McGonnigal B; Moore T; Kargupta T; Mancini RJ; Esser-Kahn AP Light guided in-vivo activation of innate immune cells with photocaged TLR 2/6 agonist. Sci. Rep 2017, 7, 8074. [PubMed: 28808328]

(20). Larson ME; Lesné SE Soluble Aβ olgiomer production and toxicity. J. Neurochem 2012, 120, 125–139.

(21). Lesné S; Koh MT; Kotilinek L; Kayed R; Glabe CG; Yang A; Gallagher M; Ashe KH A specific amyloid-β protein assembly in the brain impairs memory. Nature 2006, 440, 352–357. [PubMed: 16541076]

(22). Lendel C; Bjerring M; Dubnovitsky A; Kelly RT; Filippov A; Antzutkin ON; Nielsen NC; Härd T A hexameric peptide barrel as building block of amyloid-β protofibrils. Angew. Chem. Int. Ed 2014, 53, 12756–12760.

(23). Williams TL; Serpell LC Membrane and surface interactions of Alzheimer's Aβ peptide – insights into the mechanism of cytotoxicity. FEBS J. 2011, 278, 3905–3917. [PubMed: 21722314]

(24). Benilova I; Karran E; DeStooper B The toxic Aβ oligomer and Alzheimer's disease: an emperor in need of clothes. Nat. Neurosci 2012, 15, 349–357. [PubMed: 22286176]

(25). Measey TJ; Gai F Light-triggered disassembly of amyloid fibrils. Langmuir 2012, 28, 12588–12592. [PubMed: 22867440]

(26). Furutani M; Uemura A; Shigenaga A; Komiya C; Otaka A; Matsuura K A photoinduced growth system of peptide nanofibres addressed by DNA hybridization. Chem. Commun 2015, 51, 8020–8022.

(27). Awad L; Jejelava N; Burai R; Lashuel HA A new caged-glutamine derivative as a tool to control the assembly of glutamine-containing amyloidogenic peptides. Chem-biochem 2016, 17, 2353–2360.

(28). Johnson EGB; Lanning JD; Meredith SC Peptide backbone modification in the bend region of amyloid-β inhibits fibrillogenesis but not oligomer formation. J. Pept. Sci 2016, 22, 368–373. [PubMed: 27114096]

(29). Laganowsky A; Liu C; Sawaya MR; Whitelegge JP; Park J; Zhao M; Pensalfini A; Soriaga AB; Landau M; Teng PK; Cascio D; Glabe C; Eisenberg D Atomic view of a toxic amyloid small oligomer. Science 2012, 335, 1228–1231. [PubMed: 22403391]

(30). Spencer RK; Li H; Nowick JS X-ray crystallographic structures of trimers and higher-order oligomeric assemblies of a peptide derived from $A\beta_{17–36}$. J. Am. Chem. Soc 2014, 136, 5595–5598. [PubMed: 24669800]

(31). Do TD; LaPointe NE; Nelson R; Krotee P; Hayden EY; Ulrich B; Quan S; Feinstein SC; Teplow DB; Eisenberg D; Shea J-E; Bowers MT Amyloid β-protein C-terminal fragments: Formation of cylindrins and β-barrels. J. Am. Chem. Soc 2016, 138, 549–557. [PubMed: 26700445]

(32). Kreutzer AG; Hamza IL; Spencer RK; Nowick JS X-ray crystallographic structures of a trimer, dodecamer and annular pore formed by a $A\beta_{17–36}$ β-hairpin. J. Am. Chem. Soc 2016, 138, 4634–4642. [PubMed: 26967810]

(33). Kreutzer AG; Yoo S; Spencer RK; Nowick JS Stabilization, assembly, and toxicity of trimers derived from Aβ. J. Am. Chem. Soc 2017, 139, 966–975. [PubMed: 28001392]

(34). Salveson PJ; Spencer RK; Kreutzer AG; Nowick JS X-ray crystallographic structure of a compact dodecamer from a peptide derived from $A\beta_{16–36}$. Org. Lett 2017, 19, 3462–3465. [PubMed: 28683555]

(35). Kreutzer AG; Spencer RK; McKelly KJ; Yoo S; Hamza IL; Salveson PJ; Nowick JS A hexamer of a peptide derived from Aβ16-36. Biochemistry 2017, 56, 6061–6071. [PubMed: 29028351]

(36). Sangwan S; Zhao A; Adams KL; Jayson CK; Sawaya MR; Guenther EL; Pan AC; Ngo J; Moore DM; Soriaga AB; Do TD; Goldschmidt L; Nelson R; Bowers MT; Koehler CM; Shaw DE; Novitch BG; Eisenberg DS Atomic strucutre of a toxic, oligomeric segment of SOD1 linked to amyotrophic lateral sclerosis (ALS). Proc. Natl. Acad. Sci. U.S.A 2017, 114, 8770–8775. [PubMed: 28760994]

(37). Nelson R; Sawaya MR; Balbirnie M; Madsen AØ; Riekel C; Grothe R; Eisenberg D Structure of the cross-β spine of amyloid-like fibrils. Nature 2005, 435, 773–778. [PubMed: 15944695]

(38). Sawaya MR; Sambashivan S; Nelson R; Ivanova MI; Seivers SA; Apostol MI; Thompson MJ; Balbirnie M; Wiltzius JJW; McFarlane HT; Madsen AØ; Riekel C; Eisenberg D Atomic structures of amyloid cross-β spines reveal varied steric zippers. Nature 2007, 447, 435–457.

(39). Sievers SA; Karanicolas J; Chang HW; Zhao A; Jiang L; Zirafi O; Stevens JT; Münch J; Baker D; Eisenberg D Structure-based design of nonnatural amino-acid inhibitors of amyloid fibril formation. Nature 2011, 475, 96–100. [PubMed: 21677644]

(40). Seidler PM; Boyer DR; Rodriguez JA; Sawaya MR; Cascio D; Murray K; Gonen T; Eisenberg D Structure-based inhibitors of tau aggregation. Nat. Chem 2018, 10, 170–176. [PubMed: 29359764]

(41). Hoyer W; Grönwall C; Jonsson A; Ståhl S; Härd T Stabilaztion of a β-hairpin in monomeric Alzheimer's amyloid-β peptide inhibits amyloid formation. Proc. Natl. Acad. Sci. U.S.A 2008, 105, 5099–5104. [PubMed: 18375754]

(42). Yu L; Edalji R; Harlan JE; Holzman TF; Lopez AP; Labkovsky B; Hillen H; Barghorn S; Ebert U; Richardson PL; Miesbauer L; Solomon L; Bartley D; Walter K; Johnson RW; Hajduk PJ; Olejniczak ET Structural characterization of a soluble amyloid β-peptide oligomer. Biochemistry 2009, 48, 1870–1877. [PubMed: 19216516]

(43). Sandber A; Luheshi LM; Söllvander S; Pereira de Barros T; Macao B; Knowles TPJ; Biverstål H; Lendel C; Ekholm-Petterson F; Dubnovitsky A; Lannfelt L; Dobson CM; Härd T Stabilization of neurotoxic Alzhemier amyloid-β oligomers by protein engineering. Proc. Natl. Acad. Sci. U.S.A 2010, 107, 15595–15600. [PubMed: 20713699]

(44). Scheidt HA; Morgado I; Huster D Solid-state NMR reveals a close structural relationship between amyloid-β protofibrils and oligomers. J. Biol. Chem 2012, 287, 22822–22826. [PubMed: 22589542]

(45). Gu L; Liu C; Guo Z Structural insights into Aβ42 oligomers using site-directed spin labeling. J. Biol. Chem 2013, 288, 18673–18683. [PubMed: 23687299]

(46). Gu L; Liu C; Stroud JC; Ngo S; Jiang L; Guo Z Antiparallel triple-strand architecture for prefibrillar Aβ42. J. Biol. Chem 2014, 289, 27300–27313. [PubMed: 25118290]

(47). Huang D; Zimmerman MI; Martin PK; Nix AJ; Rosenberry TL; Paravastu AK Antiparallel β-sheet structure within the C-terminal region of 42-residue of Alzheimers β-amyloid peptides when they form 150 kDa oligomers. J. Mol. Biol 2015, 472, 2319–2328.

(48). Kreutzer AG; Nowick JS Elucidating the structures of amyloid oligomers with macrocyclic β-hairpin peptides: insights into Alzheimer's disease and other amyloid diseases. Acc. Chem. Res 2018, 51, 706–718. [PubMed: 29508987]

(49). Nowick JS; Brower JO A new turn structure for the formation of β-hairpins in peptides. J. Am. Chem. Soc 2003, 125, 876–877. [PubMed: 12537479]

(50). Spencer RK; Chen KH; Manuel G; Nowick JS Recipe for β-Sheets: foldamers containing amyloidogenic peptide sequences. Eur. J. Org. Chem 2013, 3523–3528.

(51). Zuckermann RN; Kerr JM; Kent SBH; Moos WH Efficient method for the preparation of peptoids [oligo(N-substituted glycines)] by submonomer solid-phase synthesis. J. Am. Chem. Soc 1992, 114, 10646–10647.

(52). Johnson ECB; Kent SBH Synthesis, stability, and optimized photolytic cleavage of 4-methoxy-2-nitrobenzyl backbone-protected peptides. Chem. Commun 2006, 1557–1559.

(53). Approximately 5 mg of each peptide is sufficient to perform the X-ray crystallographic and biological studies described in this paper.

(54). Spencer RK; Nowick JS A newcomer's guide to peptide crystallography. Israel J. Chem 2015, 55, 689–710.

(55). Even though peptides **1** and $\mathbf{1^{I}_{NB}}$ crystalize in similar conditions, the crystals belong to different space groups. Crystals of peptide $\mathbf{1^{I}_{NB}}$ belong to space group $P4_232$ and contain a single copy of peptide $\mathbf{1^{I}_{NB}}$ in the asymmetric unit, whereas crystals of peptide **1** belong to space group R3 and contain sixteen copies of peptide **1** in the asymmetric unit (PDB 4NTR).

(56). Peptide $\mathbf{1_{NB}}$ also grows crystals with identical morphology to those formed by peptide $\mathbf{1^{I}_{NB}}$ in these conditions, however, these crystals do not diffract X-rays. We were therefore unable to solve the X-ray crystallographic structure of peptide $\mathbf{1_{NB}}$.

(57). Peptide **2** does not assemble into the crystallographically observed hexamer at the low micromolar concentrations used in this experiment. Thus, this CD spectrum likely reflects an ensemble of folded and unfolded monomeric peptide **2**.

(58). Tam JP; Wu CR; Liu W; Zhang JW Disulfide bond formation in peptides by dimethyl sulfoxide. Scope and applications. J. Am. Chem. Soc 1991, 113, 6657–6662.

(59). Khakshoor O; Nowick JS Use of disulfide "staples" to stabilize β-sheet quaternary strucutre. Org. Lett 2009, 11, 3000–3003. [PubMed: 19534505]

(60). Foadi J; Aller P; Alguel Y; Cameron A; Axford D; Owen RL; Armour W; Waterman DG; Iwata S; Evans G Clustering procedures for the optimal selection of data sets from multiple crystals in macromolecular crystallography. Acta Crystallogr., Sect. D: Biol. Crystallogr 2013, 69, 1617–1632. [PubMed: 23897484]

(61). These conditions are similar to those used to crystalize peptides **1** and $\mathbf{1^{I}_{NB}}$.

(62). Spencer RK; Kreutzer AG; Salveson PJ; Li H; Nowick JS X-ray crystallographic structures of oligomers of peptides derived from β2-microclobulin. J. Am. Chem. Soc 2015, 137, 6304–6311. [PubMed: 25915729]

(63). Apostol MI; Perry K; Surewicz WK Crystal structure of a human prion protein fragment reveals a motif for oligomer formation. J. Am. Chem. Soc 2013, 135, 10202–10205. [PubMed: 23808589]

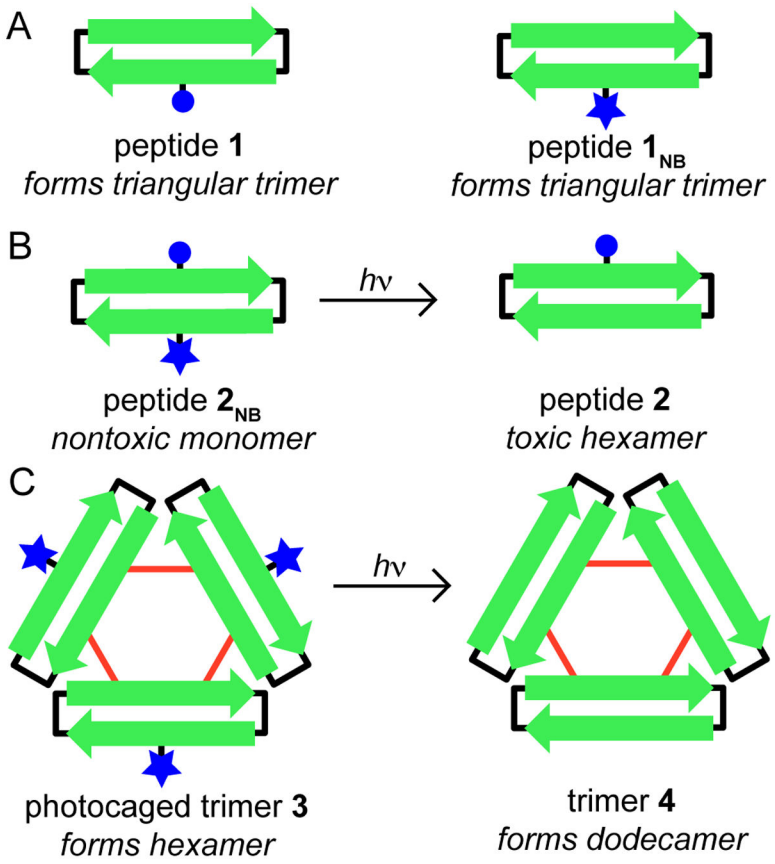

Figure 1.

Photocaged peptides derived from Aβ. (A) Replacing an *N*-methyl group (blue ball) with an *N*-2-nitrobenzyl group (blue star) does not alter the supramolecular assembly of peptide **1**. (B) Adding an *N*-2-nitrobenzyl group to peptide **2** allows its assembly and toxicity to be controlled with light. (C) Incorporating *N*-2-nitrobenzyl groups into triangular trimers allows their assembly to be controlled with light.

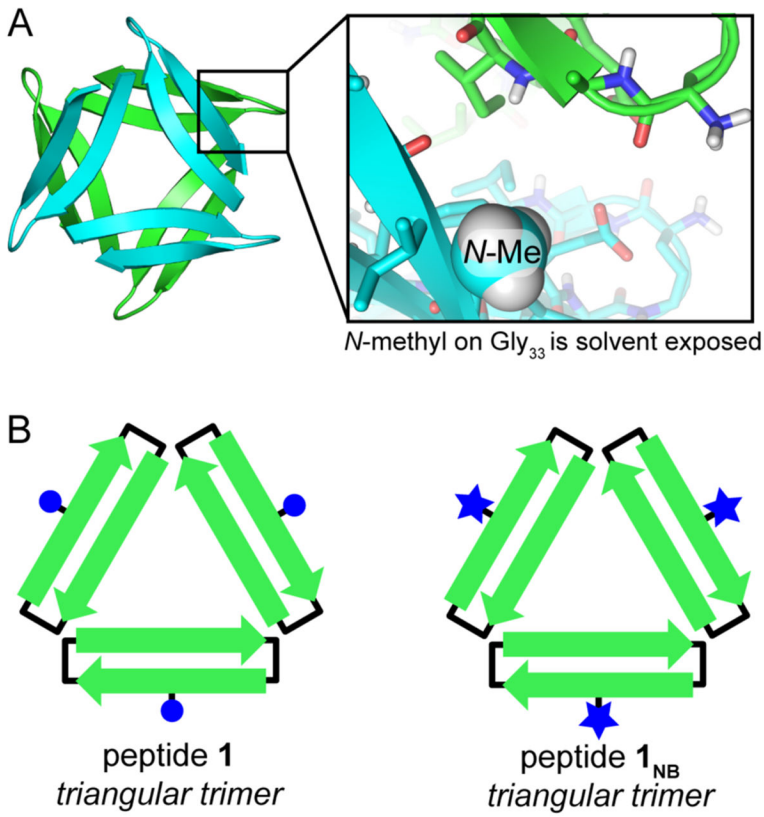

Figure 2.

Design of a photocaged homologue of peptide **1**. (A) X-ray crystallographic structure of the hexamer formed by peptide **1** (PDB 4NTR). Inset shows the position of *N*-methylglycine$_{33}$ within the hexamer. (B) Cartoon of the design of peptide $\mathbf{1_{NB}}$ in which *N*-2-nitrobenzyl groups replace *N*-methyl groups.

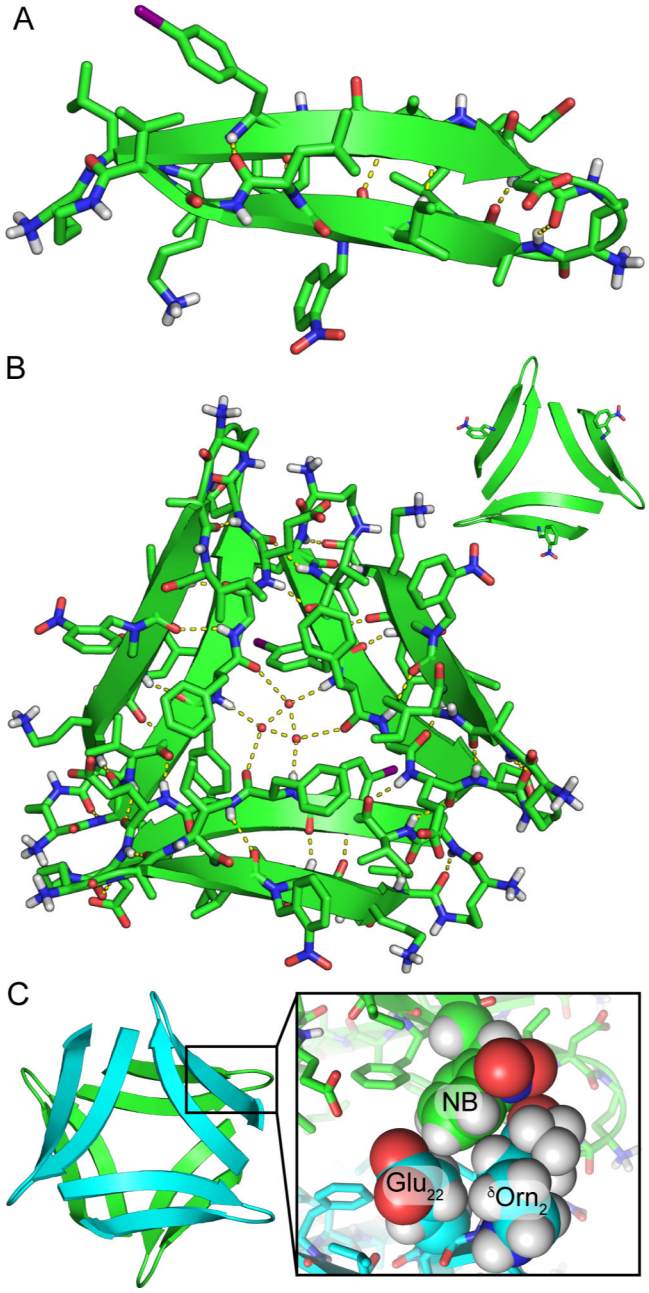

Figure 3.

X-ray crystallographic structure of peptide $\mathbf{1^{I}_{NB}}$ (PDB 6CG3). (A) The asymmetric unit contains a single, folded copy of peptide $\mathbf{1^{I}_{NB}}$. (B) Triangular trimer formed by peptide $\mathbf{1^{I}_{NB}}$. In the inset, the *N*-2-nitrobenzyl groups are shown as sticks. (C) Hexamer formed by peptide $\mathbf{1^{I}_{NB}}$ in the crystal lattice. Inset shows the inter-trimer contacts that the *N*-2-nitrobenzyl group (abbreviated NB) makes within the hexamer.

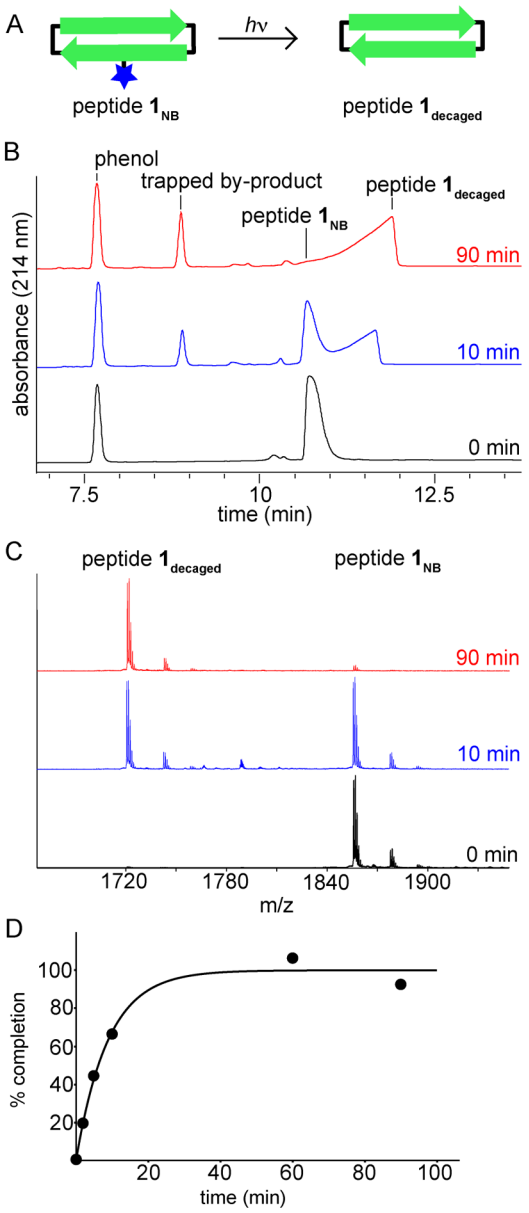

Figure 4.

Photolysis of the *N*-2-nitrobenzyl group with long-wave UV light. (A) Cartoon representation of the photolysis reaction. (B) RP-HPLC chromatograms illustrating the progress of the photolysis reaction. (C) ESI-MS illustrating the progress of the photolysis reaction. (D) Progress of the photolysis reaction monitored by RP-HPLC. The line represents a 1st-order kinetics fit of the data.

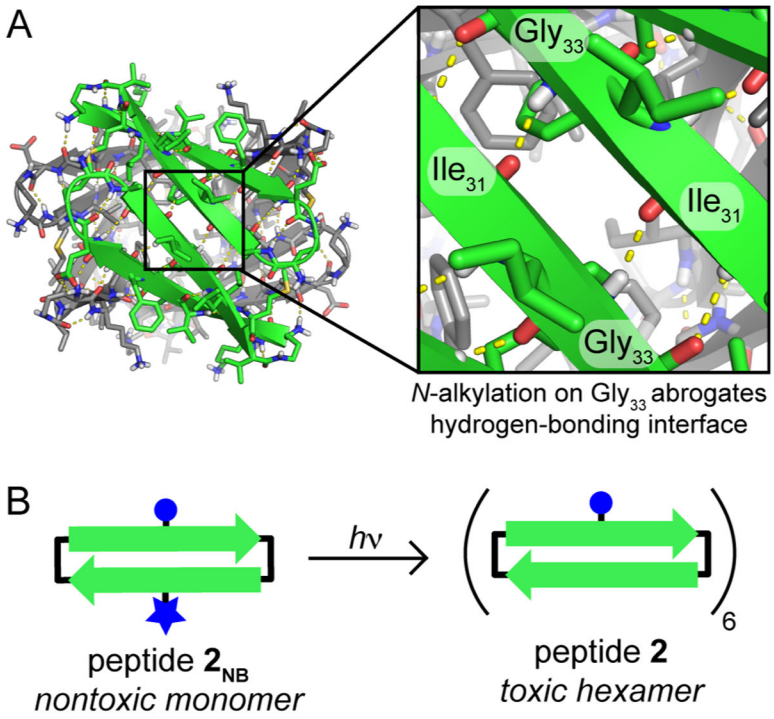

Figure 5.

Design of peptide $\mathbf{2_{NB}}$, a photocaged homologue of peptide **2**. (A) X-ray crystallographic structure of the hexamer formed by peptide **2** (PDB 5W4H). Inset shows the hydrogen-bonding interface between two neighboring monomers in which Gly_{33} hydrogen bonds with Ile_{31}. (B) Cartoon illustrating photolysis and decaging of peptide $\mathbf{2_{NB}}$ to form peptide **2**, which assembles into a toxic hexamer.

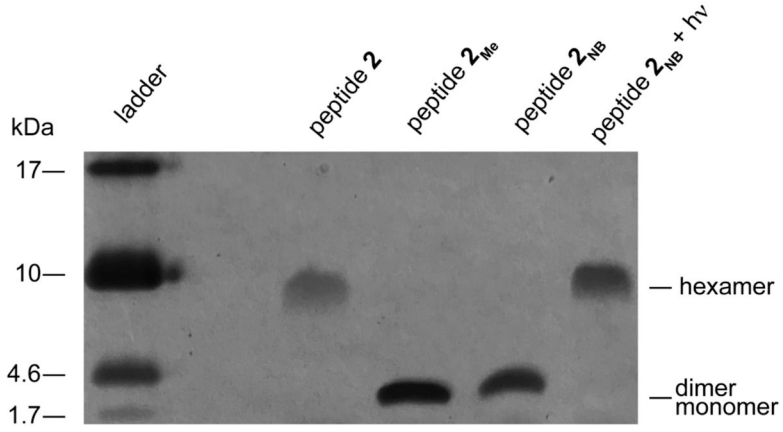

Figure 6.

An *N*-2-nitrobenzyl group alters the assembly of peptide **2**. Silver-stained tricine SDS-PAGE gel. 6 μL aliquots of 0.2 mg/mL solutions of each peptide were loaded into the lanes on the gel.

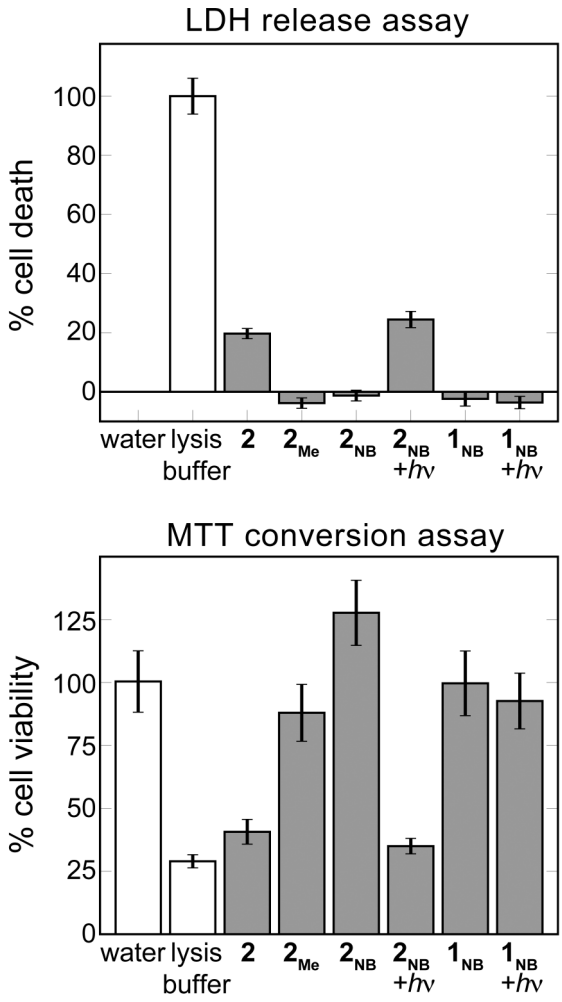

Figure 7.

An *N*-2-nitrobenzyl group alters the toxicity of peptide **2**. Toxicity of macrocyclic β-hairpin peptides towards SH-SY5Y cells as reflected in LDH release and MTT conversion assays. SH-SY5Y cells were incubated for 72 hours with 50 μM of the indicated peptide before performing the assay. Error bars represent standard deviations propagated from five replicate runs.

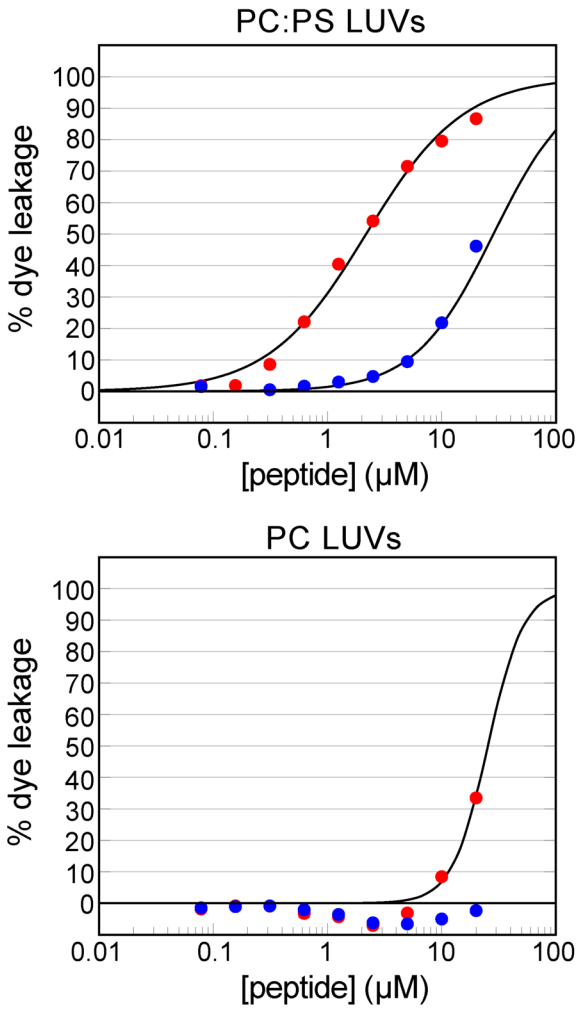

Figure 8.

Peptide **2** disrupts membrane integrity of large unilamellar vesicles. Various concentrations of peptide **2** (red) and peptide $\mathbf{2_{NB}}$ (blue) were incubated with LUVs comprising either PC:PS (1:1) or PC encapsulating 70 mM calcein. The percentage of dye leakage was monitored by the increase in fluorescence. Each point is calculated from the average of three replicate runs. Error bars (obscured by the data points) represent standard deviations propagated from three replicate runs.

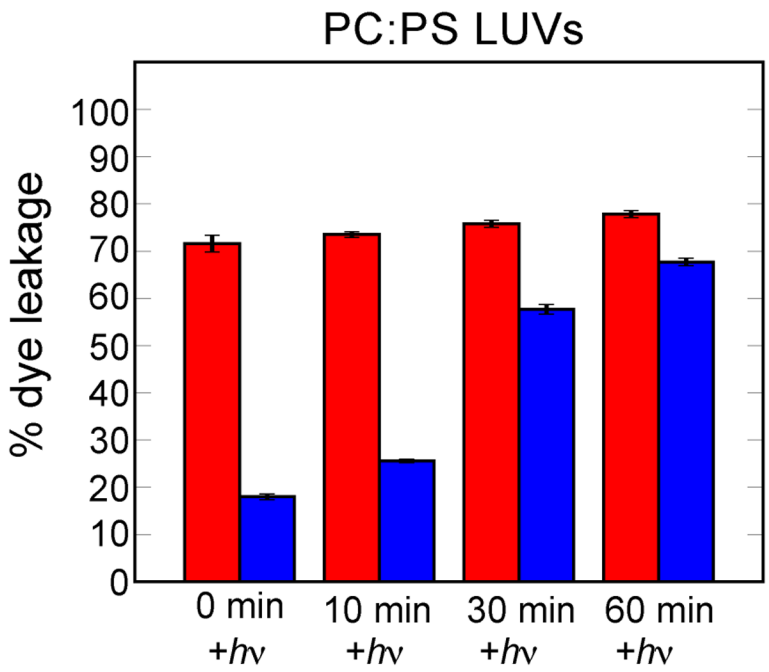

Figure 9.

Long-wave UV light restores the dye leakage activity of peptide $\mathbf{2_{NB}}$. PC:PS LUVs were incubated with 5 μM of peptide **2** (red) or peptide $\mathbf{2_{NB}}$ (blue) and irradiated with long-wave UV light. Dye leakage was assessed after 0, 10, 30, and 60 minutes of irradiation. Error bars represent standard deviations propagated from three replicate runs.

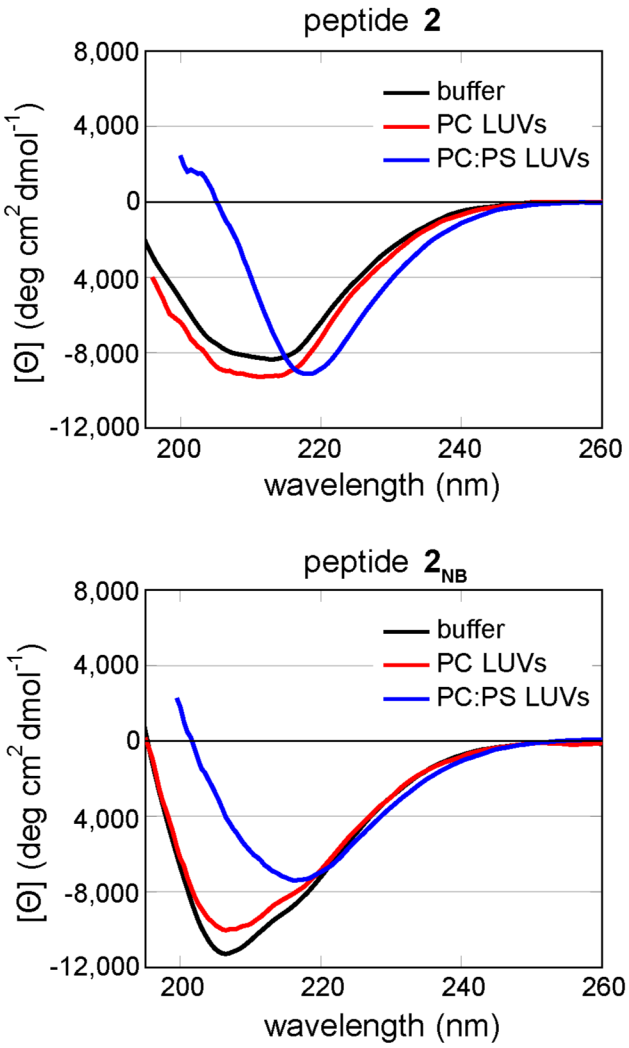

Figure 10.

Effects of liposomes on the CD spectra of peptides **2** and $\mathbf{2_{NB}}$. Spectra of 50 μM peptide in 10 mM sodium phosphate buffer at pH 7.4 were acquired in the presence or absence of 1.0 mM lipids, constituting either phosphatidylcholine (PC) or phosphatidylcholine:phosphatidylserine (PC:PS) liposomes. Data are graphed as mean residue ellipticity. The CD spectra could not be recorded below *ca.* 200 nm in the presence of the liposomes.

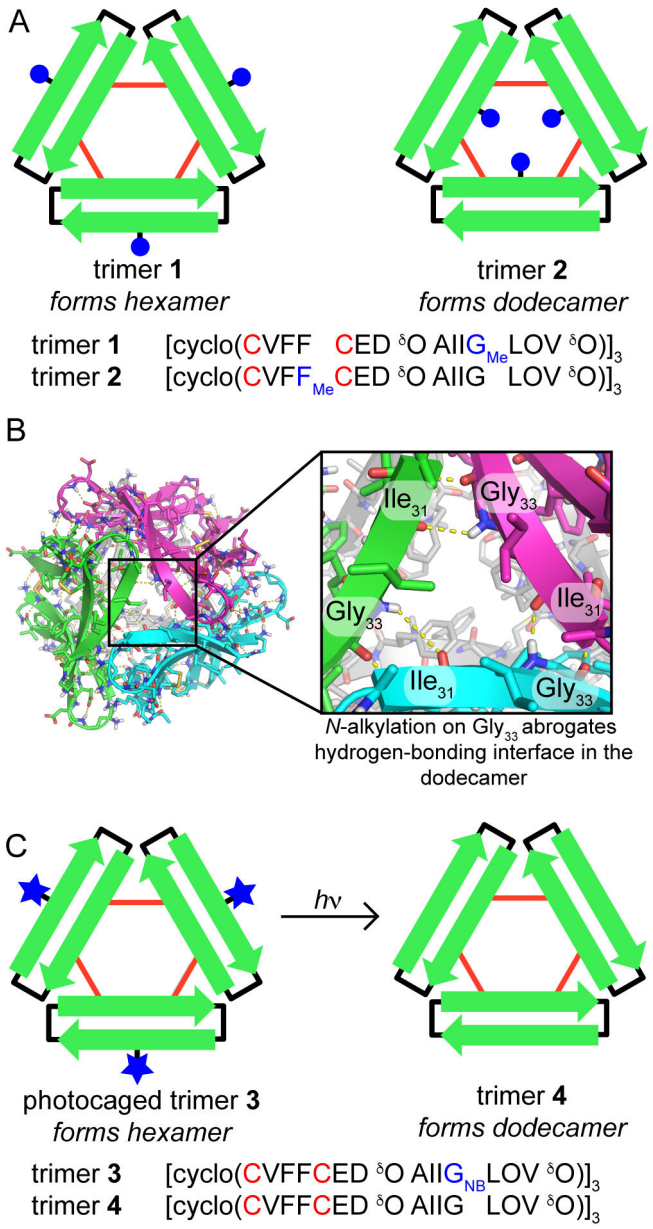

Figure 11.

Design of a photocaged triangular trimer. (A) Cartoon of two crosslinked trimers derived from peptide **1** highlighting the different positions of the *N*-methyl groups. (B) X-ray crystallographic structure of the dodecamer formed by trimer **2** (PDB 5SUR). Inset shows the hydrogen-bonding interface between three $A\beta_{30–36}$ β-strands from three neighboring trimers. (C) Cartoon illustrating the photolysis and decaging of trimer **3** to form trimer **4**.

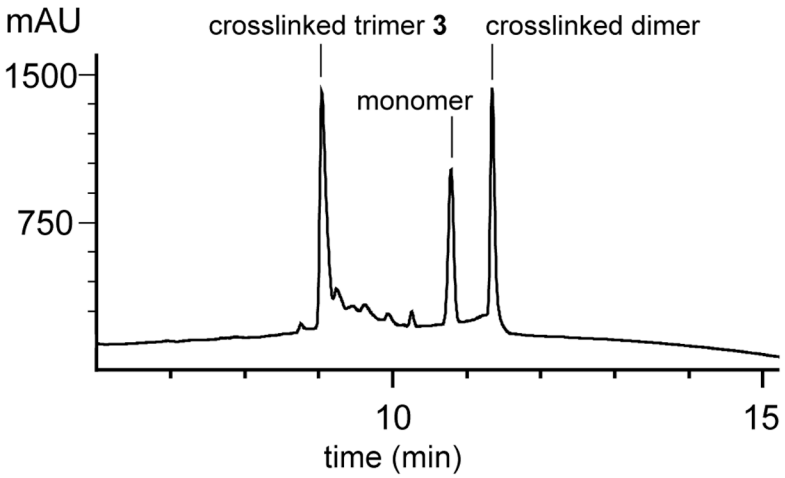

Figure 12.

Oxidation of peptide $\mathbf{3_{NB}}$ produces three major species. Analytical RP-HPLC was performed on a C18 column with an elution gradient of 5–100% CH_3CN over 20 min.

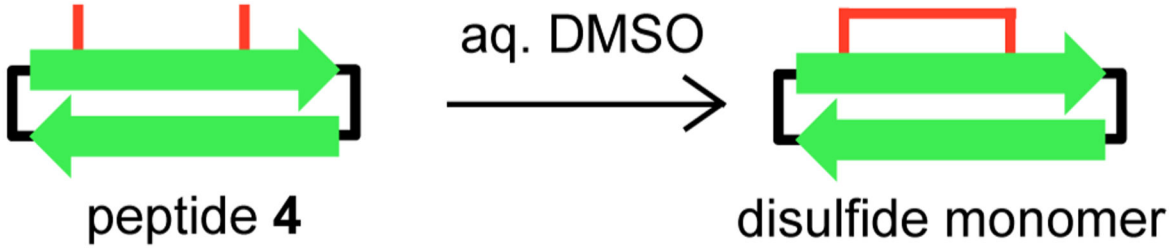

Figure 13.

Oxidation of peptide **4**, which contains neither an *N*-methyl group nor an *N*-2-nitrobenzyl group, forms only a disulfide monomer.

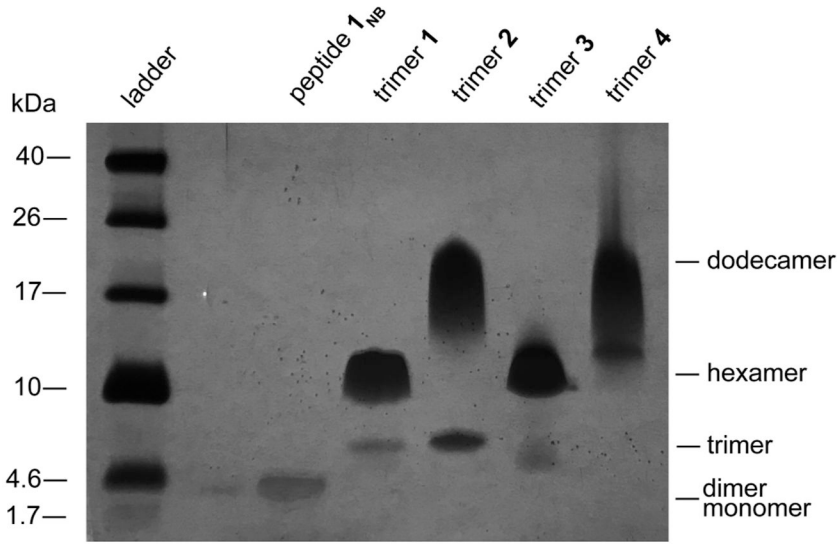

Figure 14.

Silver-stained SDS-PAGE gel illustrating the assembly of trimers **1**–**4**. 6 μL of a 0.1 mg/mL solution of each trimer was loaded into the corresponding lanes on the gel.

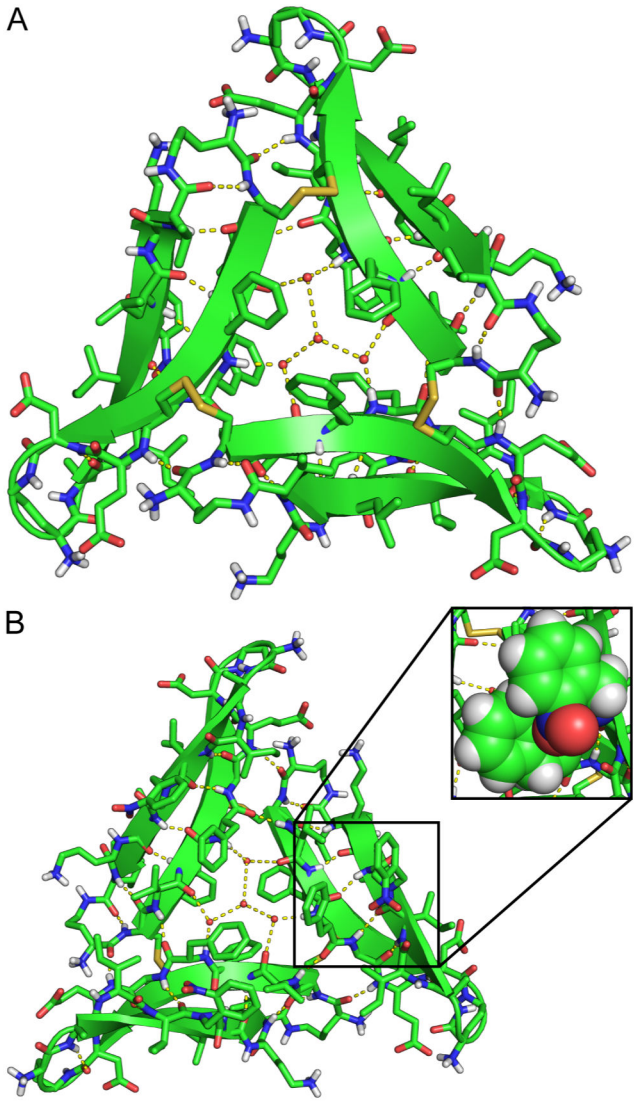

Figure 15.

X-ray crystallographic structure of photocaged trimer **3** (PDB 6CG5). (A) Top surface of trimer **3** which displays the three disulfide crosslinks. (B) The bottom surface of trimer **3** on which the three *N*-2-nitrobenzyl groups pack against Phe_{20}. In the inset, the side chain of Phe_{20} and the adjacent *N*-2-nitrobenzyl group are shown as spheres.

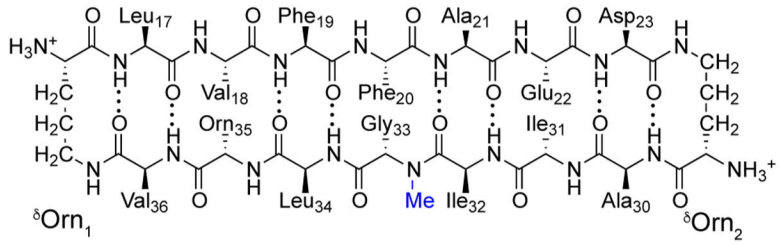

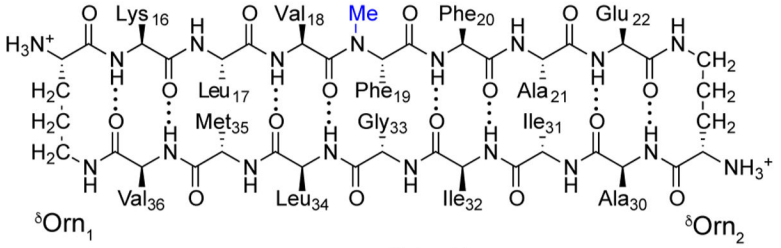

peptide **1** cyclo(LVFF AED $^{\delta}$O AIIG$_{Me}$ LOV $^{\delta}$O)

peptide **2** cyclo(KLVF$_{Me}$FAE $^{\delta}$O AIIG LMV $^{\delta}$O)

Chart 1.

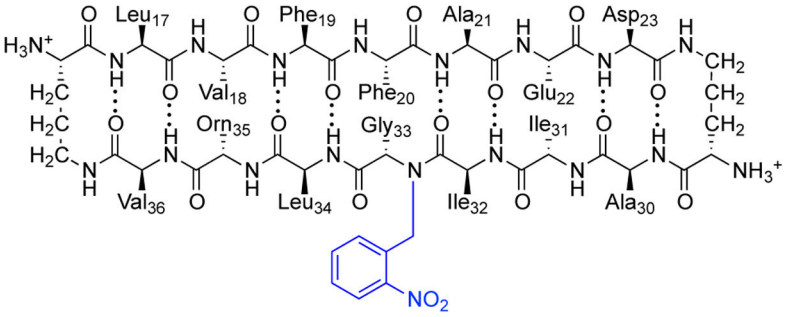

peptide $\mathbf{1}_{NB}$

peptide **1**	cyclo(LVF FAED $^{\delta}$O AIIG_{Me}LOV $^{\delta}$O)
peptide $\mathbf{1}_{NB}$	cyclo(LVF FAED $^{\delta}$O AIIG_{NB}LOV $^{\delta}$O)
peptide $\mathbf{1}^{I}_{NB}$	cyclo(LVF^{I}FAED $^{\delta}$O AIIG_{NB}LOV $^{\delta}$O)
peptide $\mathbf{1}_{decaged}$	cyclo(LVF FAED $^{\delta}$O AIIG LOV $^{\delta}$O)

Chart 2.

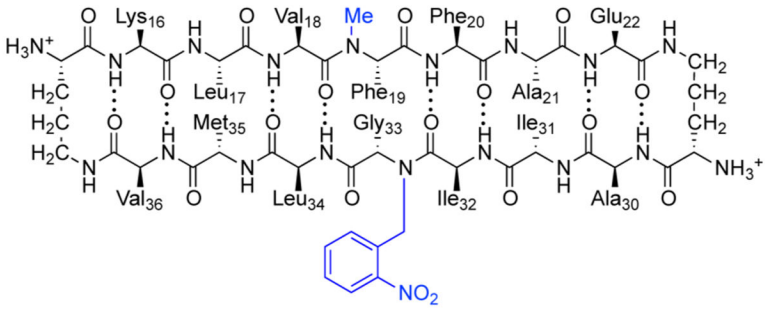

peptide $\mathbf{2_{NB}}$

peptide **2** cyclo(KLVF_{Me}FAE $^{\delta}$O AIIG LMV $^{\delta}$O)
peptide $\mathbf{2_{NB}}$ cyclo(KLVF_{Me}FAE $^{\delta}$O AIIG_{NB}LMV $^{\delta}$O)
peptide $\mathbf{2_{Me}}$ cyclo(KLVF_{Me}FAE $^{\delta}$O AIIG_{Me}LMV $^{\delta}$O)

Chart 3.

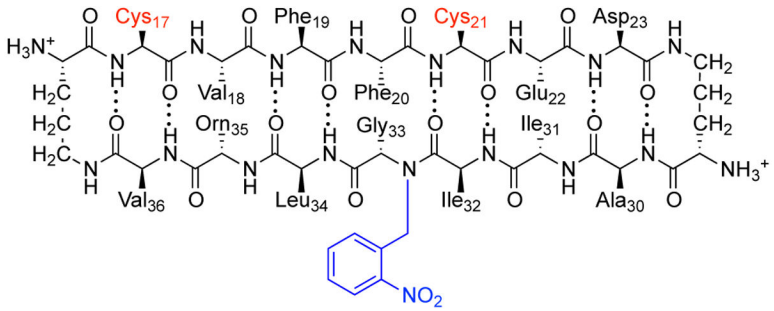

peptide $\mathbf{3}_{\mathbf{NB}}$ cyclo(CVFFCED $^{\delta}$O AIIG$_{NB}$LOV $^{\delta}$O)
peptide **4** cyclo(CVFFCED $^{\delta}$O AIIG LOV $^{\delta}$O)

Chart 4.